Available online at www.sciencedirect.com
ScienceDirect
Ceramics International 37 (2011) 2101–2107
CERAMICS INTERNATIONAL
www.elsevier.com/locate/ceramint

Structural, thermal and crystallization kinetics of ZnO–BaO–SiO_2–B_2O_3–Mn_2O_3 based glass sealants for solid oxide fuel cells

Anu Arora, Vishal Kumar, K. Singh *, O.P. Pandey

School of Physics and Materials Science, Thapar University, Patiala 147004, India

Received 17 June 2010; received in revised form 20 January 2011; accepted 27 February 2011
Available online 8 April 2011

Abstract

Glass compositions in the system $40SiO_2$–$30BaO$–$20ZnO$–$(x)Mn_2O_3$–$(10-x)B_2O_3$ glasses have been synthesized and the thermal, structural and crystallization kinetic properties characterized. The lower concentration of Mn_2O_3 in place of B_2O_3 acts as a network former and suppressed the tendency of phase separation in glasses. On the other hand, concentration of $Mn_2O_3 > 7.5$ mol% induce phase separation in the glass matrix. The highest activation energy for crystallization is observed in the composition without B_2O_3 (INM4) (355 kJ/mol). The values of thermal expansion coefficient (TEC) and viscosity of this glass is 8×10^{-6} K^{-1} and $10^{4.2}$dPa s (850 °C), respectively. After long heat treatment (800 °C for 100 h), thermodynamically stable hexacelsian and monoclinic phases are formed. These phases are not detrimental to SOFC application.

Keywords: Scanning electron microscopy; X-ray diffraction; Fuel cells; Glass

1. Introduction

In recent time, many researchers have reported that glasses and glass ceramics can be used as sealing materials for solid oxide fuel cell (SOFC). However, the development of a suitable sealant for planar design of SOFC is a very challenging task. Conventional sealing materials cannot work at the operating temperature of SOFC. Thus, glass and glass ceramics are most suitable candidates for sealing at a high temperature with other stringent conditions, which is required for SOFC operation [1–6]. Glass ceramics have superior mechanical properties along with other properties. Basically, glass can be converted in glass ceramics by controlled heat treatment above glass transition temperature (T_g) [7]. The segregation of different crystalline phases from the glass matrix affects the properties of the glasses. These properties are influenced by the volume fraction of crystalline phases and their chemical nature. Lara et al. [8] have investigated ZnO containing glasses and reported that thermal expansion coefficient (TEC) of these glasses in the range of other components of SOFC. Moreover, it shows very small change in the thermal expansion with respect to temperature as compared to Ca and Mg containing glasses. Moreover, the addition of ZnO increases the glass forming range. Glass transition (T_g) and softening temperatures (T_s) decrease with increasing ZnO content in the zinc silicate glass [6]. Wang et al. [9] concluded that glasses containing ZnO showed good adherence with yttria stabilized zirconia (YSZ) which is used as an electrolyte in SOFC. The objective of the present study is to investigate the effect of Mn_2O_3 on physical, thermal and crystallization kinetics of SiO_2–B_2O_3–BaO–ZnO glass so that these properties can be explored for SOFC applications. The selection of Mn_2O_3 as an intermediate oxide was based on its variable oxidation states. Moreover, until date nobody has reported the effect of Mn_2O_3 on various sealing properties of above glass and glass ceramics. The kinetics of crystallization has been evaluated using differential thermal analysis and dilatometer studies. The crystalline phases in the heat treated glasses were identified by X-ray diffraction. The morphologies of crystal growth and elemental analysis were done by scanning electron microscope and energy dispersive spectroscopy (EDS), respectively.

2. Experimental procedure

Zinc barium silicate (ZBS) glass compositions with their labels are listed in Table 1. The raw materials taken were SiO_2,

* Corresponding author.
E-mail address: kusingh@thapar.edu (K. Singh).

0272-8842/$36.00
doi:10.1016/j.ceramint.2011.02.027

Table 1
Glass composition in mol%.

Glass sample	SiO_2	BaO	ZnO	B_2O_3	Mn_2O_3
INM1	40	30	20	7.5	2.5
INM 2	40	30	20	5.0	5.0
INM3	40	30	20	2.5	7.5
INM4	40	30	20	0	10

B_2O_3, Mn_2O_3, BaO and ZnO (Sigma Aldrich). The purity of the oxides was ≥99.9 mol%. The mixture was ground to break agglomerate particles. After agate mortar pestle grinding, the mixture was transformed to ball mill and ground for two hours (h) in a wet medium (acetone). The ball milling was done using porcelain balls in a porcelain jar (Retsch, Germany, Model S 1000). The mass to ball ratio for system was 1:2. The resulting mixture was dried in the air. The mixed dried powder of the homogenous mass was transformed in recrystallized alumina crucible and heated in an atuomized Molybdenum Disilicide ($MoSi_2$) electric high resistance furnace. The batches were heated at 1550 °C and kept at this temperature for 2 h in order to achieve the homogeneous molten glass. The quenching of molten mass was done on flat copper plates. The obtained glasses were annealed at 500 °C (below T_g) for 10 h to remove the internal stresses generated during quenching process. Thermal expansion coefficient (TEC), T_g and T_d were measured using a Netzsch (DIL 402 PC) dilatometer. The annealed sample was cut to a specific length as per the requirement of an apparatus and heated at a rate of 5 °C min^{-1} from room temperature to 700 °C in air atmosphere. The value of viscosity is calculated by using the values of T_g and T_s obtained from dilatometer.

Crystallization kinetics of the glass were studied by differential thermal analysis (DTA) using a Perkin-Elmer (Diamond TG/DTA) system. The DTA measurement was performed using different heating rates (10, 20, 30, 40 °C min^{-1}) in an N_2 atmosphere. The values of T_g, T_c and T_{pc} were obtained from DTA thermogram and these values were used to calculate a crystallization activation energy (E_a), thermal stability parameter (S) and fragility index (F).

After confirming the amorphous nature of as prepared glass, some glasses were heat treated at 800 °C for various time intervals. The crystalline phases were identified by X-Ray diffraction (XRD) using a Philips Xpert powder diffractometer with monochromatic CuK_α radiation at a scan speed of 1° min^{-1}. These base glass and heat treated samples were mounted in epoxy, ground and polished to a mirror like finish. After polishing, the samples were lightly etched with HF and coated by silver to reveal a crystalline microstructure. The microstructures were observed using EVO 50 scanning electron microscope (SEM).

3. Results and discussion

3.1. Thermal Analysis

The obtained T_g, T_c and T_{pc} of present glasses is given in Table 2. The DTA curves of all the glasses were exhibiting two exothermic peaks as shown in Fig. 1. However, these peaks are not fully resolved. As the percentage of Mn_2O_3 increases (up to >7.5 mol%) in the glasses, the exothermic peaks become sharp, which indicates the lower phase separation tendency in these glasses. This may be attributed that up to 7.5 mol% Mn_2O_3 in glass is working as a glass former. It is well reported in the literature that the intermediate oxides can act either as a glass former or glass modifier [10]. Fig. 1 shows DTA plot of INM4 glass powder at different heating rate. The DTA curves corresponding to heating rate 10, 20, 30 and 40 °C min^{-1} show presence of two exothermic peaks. These exothermic peaks indicate crystallization of $BaAl_2Si_2O_8$ and Ba_2MnO_3 phases. These phases crystallized in heat treated glass as shown in Fig. 7.

Table 2
Activation energy (E_a), glass transition (T_g), crystallization (T_c) and peak crystallization temperature (T_p) of glass samples.

Sample labels	T_g	T_c	T_{pc}	E_a (kJ mol^{-1})
INM1	676	791	806	315
INM 2	685	780	829	281
INM3	699	790	833	200
INM4	666	757	780	355

Furthermore, the phase separation in base glasses is also observed which is described in last section. Basically, it depends on coordination of cations and anions in the glass matrix. In the present glass series, INM4 (x = 10) samples show a higher tendency of the phase separation along with lower values of T_g, T_c and T_{pc} as shown in Table 2. In other words, a phase separation tendency suppresses in those glasses where B_2O_3 and Mn_2O_3 both are present. It means competition between B^{3+} and Mn^{3+} cations leads to increase T_g and suppress phase separation. Phase separation phenomena can be explained on formation of nucleation sites at different places in the glass matrix with increasing contents of the glass modifier. Due to different sites, phases in the matrix have different kinetics that induced phase separation [11].

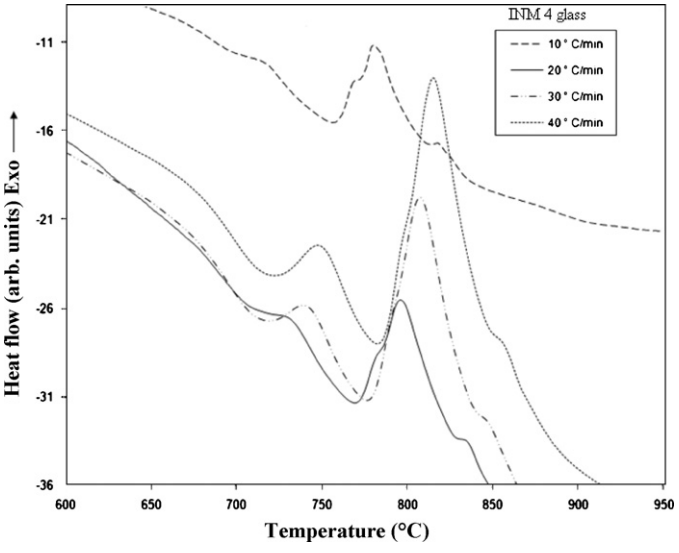

Fig. 1. DTA plot of glass powder at 10, 20, 30, 40 °C/min from 600 to 1000 °C.

3.1.1. Thermal stability parameter (S)

A parameter (S) usually employed to estimate the thermal stability (ΔT) of glass [12], is defined by the following equation.

$$\Delta T = T_c - T_g \quad (1)$$

The bigger difference between T_c and T_g indicates the most thermally stable glass.

Saad and Poulain [13] obtained another criterion, the thermal stability parameter:

$$S = \frac{(T_p - T_c)(T_c - T_g)}{T_g} \quad (2)$$

Its value reflects the resistance to devitrification after the formation of the glass. In Eq. (2), $(T_p - T_c)$ is related to the rate of devitrification transformation of the glassy phases. On the other hand, a high value of $(T_c - T_g)$ delays the nucleation process. In the present glasses, pure glass INM4 exhibit higher thermal stability than other glasses as shown in Fig. 2. The presence of intermediate oxide Mn_2O_3, along with B_2O_3 weaken the glass network and enhance crystallization.

3.1.2. Fragility index (F)

Structural relaxation is a general phenomenon occurring when a glass is maintained at a temperature below its glass transition temperature (T_g). Glass forming liquids that exhibit an approximately Arrhenius temperature dependence of the viscosity are defined as strong glass formers and those, which exhibit a non-Arrhenius behavior is declared fragile glass formers [14]. Fragile glasses are usually substances with non directional, interatomic/intermolecular bonds. Strong glasses are those which show resistance to structural degradation in the liquid state.

The fragility index values with Mn_2O_3 percentages are also shown in Fig. 2. These values are calculated using the following relation [15,16]:

$$F = \frac{E_t}{RT_g \ln 10} \quad (3)$$

where E_t is the activation energy for glass transition.

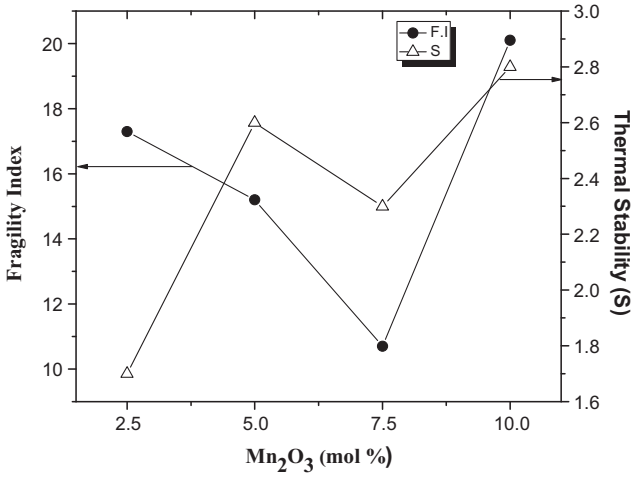

Fig. 2. Plot of Mn_2O_3 (mol%) vs. fragility index and thermal stability.

It was found that the limit for kinetically strong-glass-forming (KS) liquids is reached for a low value of F ($F \approx 16$) [17], while the limit for kinetically fragile-glass-forming (KF) liquids is characterized by a high value of F ($F \approx 200$) [18]. It is observed that INM1 composition has the strongest glass forming liquids among all the four glasses.

The strong glass forming tendency in INM1 glass might be due to highest mol% of B_2O_3 (glass former) compared to INM2 and INM3. As the mol% of B_2O_3 is decreased the fragility index also decreases. It indicates B_2O_3 might be playing an important role to form strong glass forming liquids. However, in case of INM4 glass B_2O_3 is completely replaced by Mn_2O_3 which itself starts acting as glass former and improves the fragility index [10]. INM2 and INM3 are kinetically fragile-glass-forming (KF) liquids probably due to the competition between B_2O_3 and Mn_2O_3 to form an independent glass network.

3.2. Calculation of viscosity of glasses from dilatometer data

According to the simple liquid theory (Mott and Gurney) [19], there is a relationship between pseudo-critical temperature (T_k) and the absolute melting point (T_m):

(5) $\frac{T_k}{T_m} = \frac{2}{3}$

Beaman [20] proved that this rule can be applied on the glass systems of molecular compounds and polymers, and it is also suitable for the inorganic compound glasses. So, it can be used by replacing T_m with liquid temperature (T_l) and T_k by glass transition temperature (T_g). Thus, the rule can be presented as [21]:

$$\frac{T_g}{T_l} = \frac{2}{3} \quad (5)$$

The viscosity values at T_g, dilatometer softening temperature (T_d) and T_m are fixed and independent of materials [22].

$$T_g \rightarrow \eta_g = 10^{12}\ \text{Pa s}$$

$$T_s \rightarrow \eta_s = 10^{6.6}\ \text{Pa s}$$

$$T_m \rightarrow \eta_m = 10^{4}\ \text{Pa s} \quad (6)$$

Then according to the Vogel–Fulcher–Tamman (VFT) equation [23]:

$$\log \eta = A + \frac{B}{T - T_0} \quad (7)$$

where A, B and T_0 are constants. Using the parameters in Eq. (7), the constants can be obtained by resolving coupled equations for the investigated glasses. From dilatometer data values of thermal expansion coefficient (TEC), transition temperature (T_g), dilatometer softening temperature (T_s) and viscosity is obtained.

The transition point (T_g) and the softening point (T_d) of the investigated glass as calculated from the dilatometric curve were found to be 535 °C and 575 °C, respectively. The thermal expansion coefficient (TEC) of the glass was calculated as

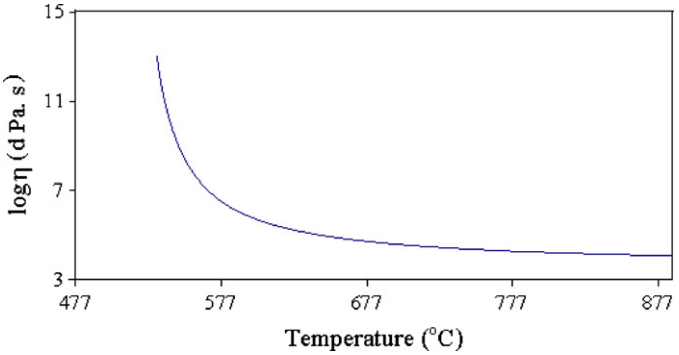

Fig. 3. Plot of log η vs. temperature.

$8 \times 10^{-6}\ ^{\circ}C^{-1}$ from the slope of the linear part of a thermal expansion curve (i.e. 200–600 °C). The thermal expansion of present glass samples is very close to required value for the sealant. By using the values of T_g and T_s obtained from dilatometry, VFT equation for the glass is derived to be:

$$\log \eta = 3.55 + \frac{190.97}{T - 785.55} \quad (8)$$

The viscosity–temperature curves of the glass calculated with Eq. (8) is shown in Fig. 3.

The viscosity value of Mn_2O_3 containing glass is calculated at 800 °C. The value of viscosity is $\sim 10^{4.2}$ dPa s. It is lower than the required viscosity value for sealing application [24].

3.3. Activation energy for crystallization

The effect of heating rate on the peak crystallization temperature (T_{pc}) in typical DTA thermograph is shown in Fig. 1. The figure shows DTA curves for INM4 glass powders at heating rates of 10, 20, 30 and 40 °C min^{-1}. The DTA curve obtained at heating rate of 10 °C min^{-1} shows two crystallization peaks at 715 and 770 °C. These two exothermic peaks correspond to crystallization of $BaAl_2Si_2O_8$ and Ba_2MnO_3 phases respectively in the glass matrix. It is observed that with increase in heating rate T_{pc} increases. T_{pc} in DTA scans corresponds to the temperature at which rate of transformation of the viscous liquid into crystal becomes maximum. The number of nucleation site is increased, by using slower heating rates, the peak maximum will occur at which melt viscosity is higher (at lower temperature). This explains the increase in T_{pc} with the increase in heating rate.

Glass transition temperature increases with substitution of Mn_2O_3 in place of B_2O_3 as is evident in Fig. 4. However, the T_g decreases when B_2O_3 is completely replaced by the Mn_2O_3 in glass composition. This can be explained on the basis of various oxidation states of Mn cation. Initially, Mn cation exhibits Mn^{4+} oxidation states in the glass matrix and act as a network former. This results in higher cross link density of cation in the glass matrix [25]. Apart from this, higher oxidation states of Mn cations convert the non bridging oxygen into bridging oxygen. Conclusively, the addition of Mn_2O_3 increased the connectivity of glass network up to 7.5 mol% of Mn_2O_3. Above this Mn_2O_3 remains in a lower oxidation state (say Mn^{3+}) and acts as a glass

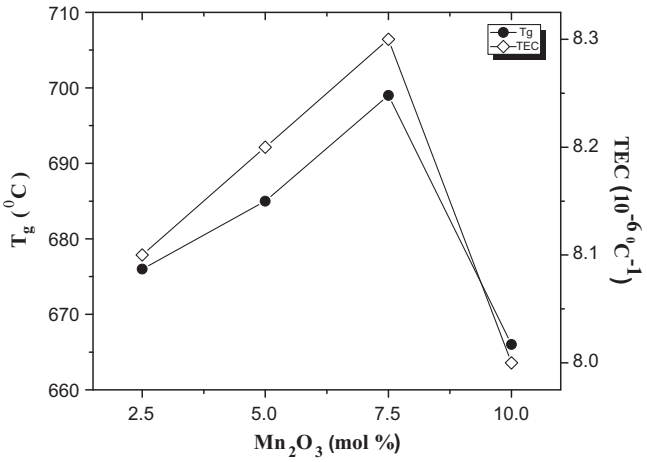

Fig. 4. Plot of Mn_2O_3 (mol%) vs. T_g and TEC.

modifier. Due to this reason, the tendency of phase separation is increased. Many researchers [11,26] have also reported that intermediate oxides could be acting as either network former or network modifier that depends on their percentage in glass composition. For the evaluation of activation energy for crystallization (E_c) using the variation of T_{pc} with β Vázquez et al. [27] developed a method for non-isothermal analysis of devitrification as follows:

$$\ln[T_p^2/\beta] = E_c/RT_p + \ln q \quad (9)$$

where q is the pre-exponential factor, β is heating rate and R is gas constant. From the experimental data, a plot of $\ln(T_p^2/\beta)$ vs. $1/T_p$ has been drawn at each heating rate, and also the straight regression line shown in Fig. 5 for each peak. It is possible to deduce the value of the activation energy, E_a = 355 kJ mol^{-1} from the slope of this experimental straight line (Eq. (9)). The activation energy for crystallization is observed to be less than our earlier studies where intermediates oxides are completely absent [28]. It can be explained on the basis of field strength of B^{3+} and Mn^{3+}. The field strength of B^{3+} is higher than Mn^{3+} cation.

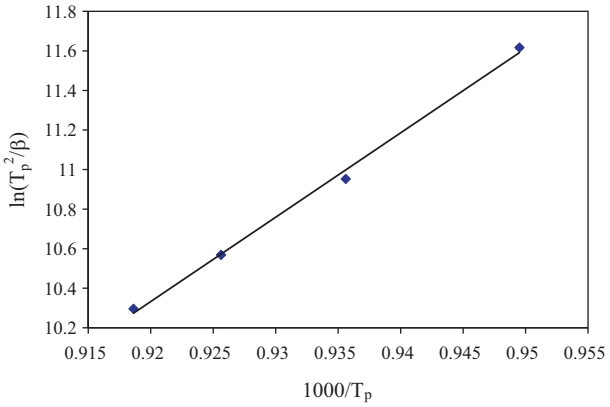

Fig. 5. Plot of $\ln(T_p^2/\beta)$ vs. $10^3/T_p$ of glass powder.

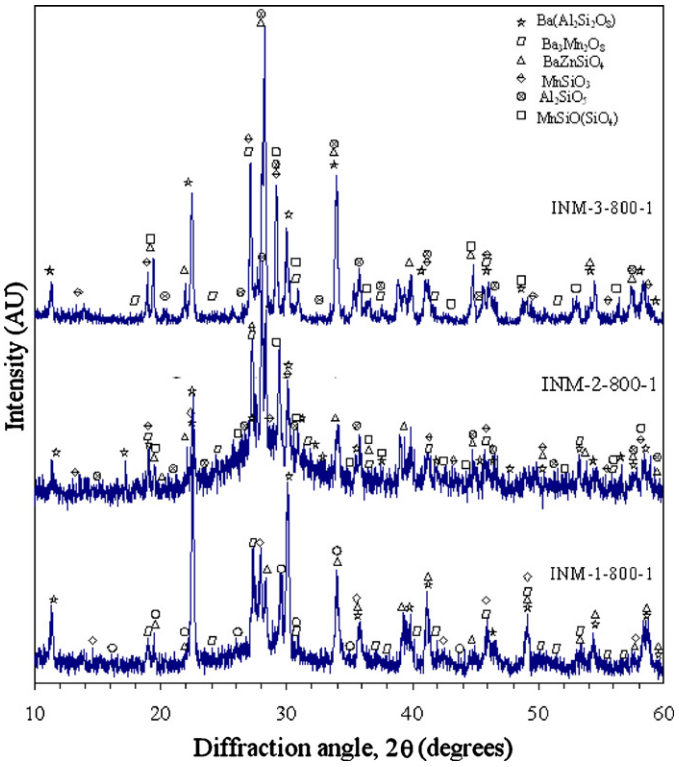

Fig. 6. XRD pattern of INM1, INM2 and INM3 glass heat-treated at 800 °C for 1 h.

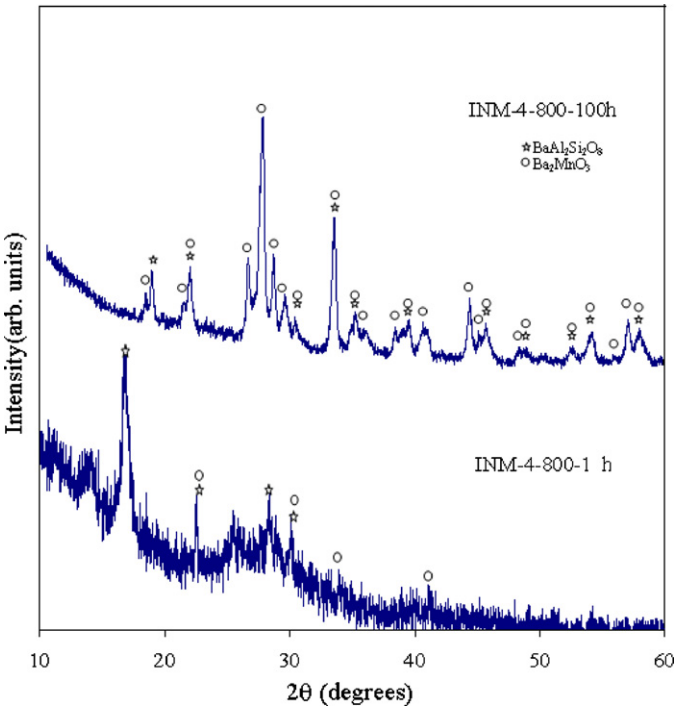

Fig. 7. XRD pattern of INM4 glass heat-treated at 800 °C for 1 and 100 h.

3.4. X-ray analysis

When glass samples are heat-treated for 1 h various crystalline phases are formed. The X-ray diffraction patterns obtained during heat-treatment of 1 h for INM1, INM2 and INM3 glasses are given in Fig. 6. All three glasses have shown nucleation of $Ba(Al_2Si_2O_8)$, $Ba_3Mn_2O_8$, $BaZnSiO_4$, $MnSiO_3$, Al_2SiO_5 and $MnSiO(SiO_4)$ phases.

However, in case of INM4 glass extent of crystallization is relatively less as compared to other three glasses. When this glass sample is heat treated at 800 °C for 1 h only hexagonal $BaAl_2Si_2O_8$ (ICDD card number 77-185) and monoclinic Ba_2MnO_3 (ICDD card no. 72-0193) crystalline phases are formed as shown in Fig. 7. In order to check the thermal stability of these phases INM4 glass was heat treated for 100 h at 800 °C. Even after long heat treatment of 100 h the glass matrix is not changing and shows formation of hexagonal $BaAl_2Si_2O_8$ and monoclinic Ba_2MnO_3 only.

Formation of polymorphs of barium aluminum silicate is unexpected as no Al_2O_3 was incorporated in initial glass composition. Evidently, chemical interactions between alumina and the glass melt took place due to unavoidable uptake of the former from the crucible during melting. EDS analysis of the glass frits confirmed the presence of alumina in the amount of 5–7 wt% and ZnO 16 wt%, whereas no deviation was observed for other constituents of glass. The unexpected result is also confirmed by wet chemical analysis. It also confirmed the observed variation in the composition of glass for Al_2O_3 and ZnO (6% and 15%, respectively) and no variation was observed for SiO_2, BaO and B_2O_3. Interestingly, in heat treated glass, B_2O_3 and ZnO could not form any crystalline phase. It is well known phenomenon in silicate glasses that during an early stage of heat treatment SiO_2 rich phases nucleate and in later stage of heat treatment other cations dissolve and form more stable crystalline phases [29].

3.5. SEM analysis

SEM analysis of room temperature aged base glass was done to understand the phase separation mechanism. In order to understand this phenomenon, a zone was located where formation of crack can be seen. This was required as phase separation can lead to generation of strain causing crack. Fig. 8 depicts such area. The EDS analysis done near the crack zone

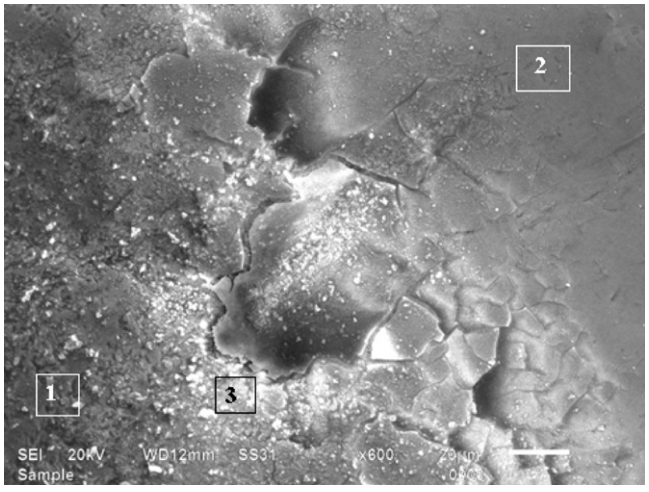

Fig. 8. SEM micrograph of INM-4 as prepared glass.

Table 3
Elemental analysis at point 1, 2 and 3 in Fig. 8.

	Element	wt%	at%
Point 1	O K	11.31	38.70
	Si K	9.39	18.29
	Mn K	4.08	4.07
	Zn K	20.46	17.13
	Ba K	54.75	21.82
Point 2	O K	14.92	46.64
	Si K	8.42	14.99
	Mn K	3.53	3.22
	Zn K	21.24	16.25
	Ba K	51.89	18.90
Point 3	O K	3.03	15.16
	Si K	6.41	18.23
	Mn K	3.08	4.48
	Zn K	17.52	21.42
	Ba K	69.96	40.71

(marked 3) gives different composition as compared to other areas (marked as 1 and 2) which is given in Table 3. The variation in compositions at near crack point as compared to other areas indicate the presence of two types of matrix in the glass. One corresponds to barium rich and other for barium less. Since the XRD analysis indicate that glass is amorphous so that variation in composition is only due to phase separation in glass. Fig. 9 (a and b) shows the SEM images of glass sample when it is heat treated at 800 °C for 10 h time duration at a low and high magnification. It is clear from these micrographs that nucleation of crystalline phases in the glass matrix have occurred. These phases are uniformly distributed throughout the glass matrix. The crystallite size is observed to vary from 2 μm to 8 μm. These nucleated phases are faceted in nature,

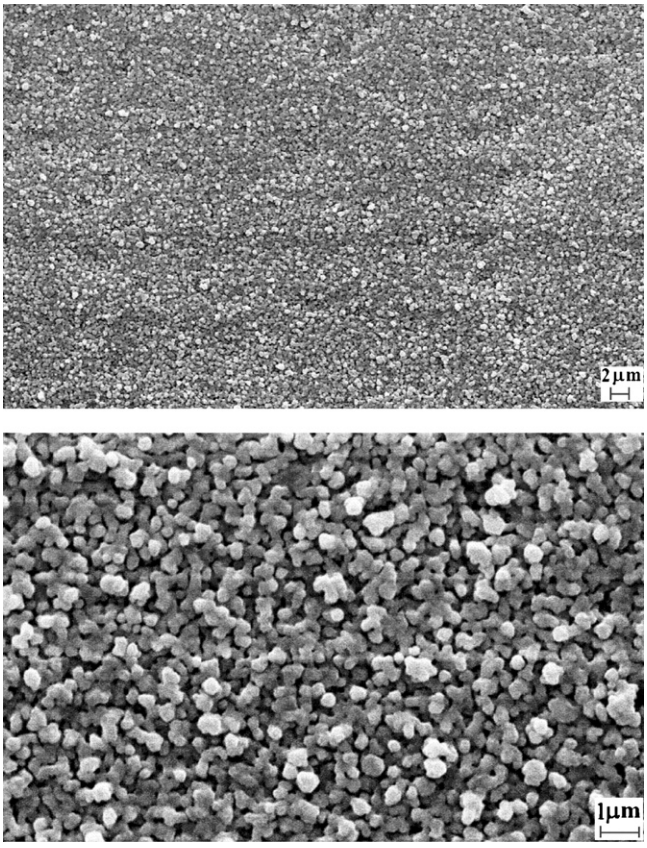

Fig. 9. (a and b) SEM micrograph of INM-4 glass heat treated at 800 °C for 10 h.

which is a typical characteristic of brittle substances. The important features observed are that all the nucleated phases grow uniformly in all the direction. The polygonal phases grow first in the close packed direction at different planes. The

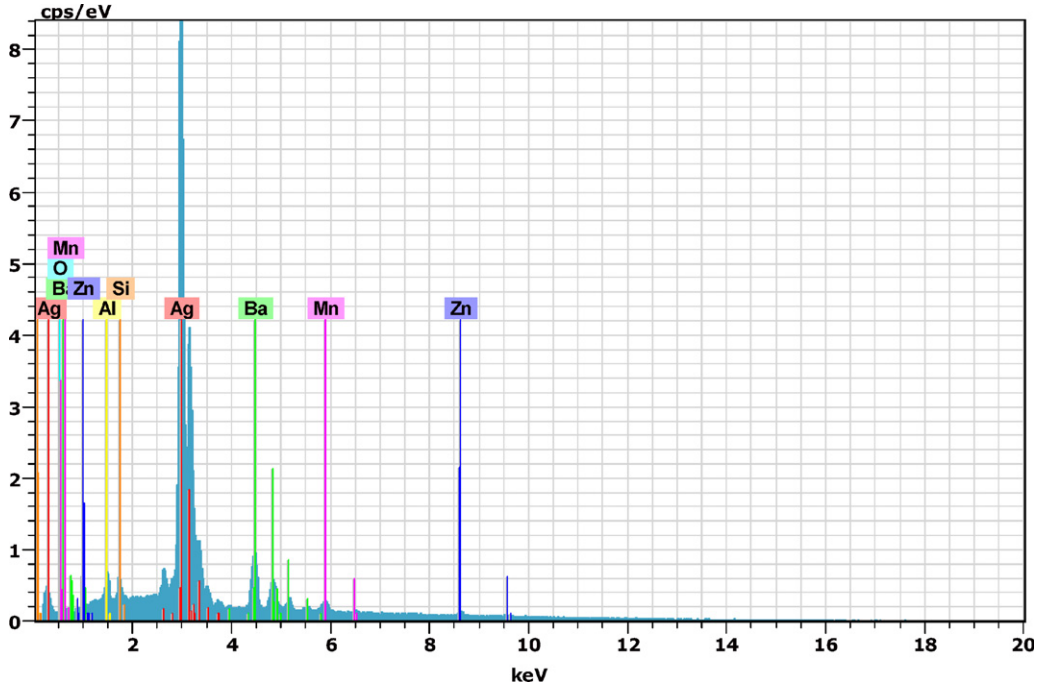

Fig. 10. EDS analysis of polished glass frit heat-treated at 800 °C for 10 h.

faceted hexagonal features are of hexagonal barium aluminum silicate ($BaAl_2Si_2O_8$) as can be seen in the structure. The EDS analysis done on the selected area of 10 h heat-treated glass sample indicates the presence of hexagonal $BaAl_2Si_2O_8$ and monoclinic Ba_2MnO_3 phases. The EDS graph (Fig. 10) also showed the presence of silver, which is due to coating of the silver on the surface of the tested sample.

4. Conclusions

The addition of Mn_2O_3 leads to increase the glass transition temperature, crystallization temperature of the glasses up to 7.5 mol%. Higher percentage of Mn_2O_3 (10 mol%) leads to decrease the glass transition temperature along with induced phase separation. The TEC of present glass is within a required limit for SOFC. The value of fragility index, F indicates that the glass is formed from a kinetically stable liquid. Activation energy of INM4 glass is 355 kJ/mol.

Acknowledgement

Authors are very grateful to Department of Science and Technology, Govt. of India for providing the financial support under the research scheme SR/S2/CMP-48/2004. One of the authors Vishal Kumar is grateful to CSIR for providing financial support.

References

[1] S. Mitachi, R. Nagase, Y. Takeuchi, R. Honda, Durable glass ceramic ferrule for general telecommunication use, Glass Technol. 39 (1998) 98.
[2] P.W. McMillan, G. Partridge, The dielectric properties of certain ZnO-Al_2O_3-SiO_2 glass-ceramics, J. Mater. Sci. 7 (1972) 847.
[3] P.W. McMillan, G. Partridge, F.R. Ward, Glass-ceramics for the coating and bonding of silicon semiconductor material, J. Mater. Sci. 4 (1969) p634.
[4] C. Lara, M.J. Pascual, R. Keding, A. Durán, Electrical behavior of glass-ceramics in the systems RO–BaO–SiO_2 (R = Mg Zn) for sealing SOFCs, J. Power Sources 157 (2006) 377.
[5] M.J. Pascual, V.V. Kharton, E. Tsipis, A.A. Yaremchenko, C. Lara, A. Durán, J.R. Frade, Transport properties of sealants for high-temperature electrochemical applications: RO-BaO-SiO_2 (R = Mg, Zn) glass-ceramics, J. Eur. Ceram. Soc. 26. (2006) 3315.
[6] C. Lara, M.J. Pauscal, A. Duran, Glass-forming ability, sinterability and thermal properties in the systems RO-BaO-SiO_2 (R = Mg, Zn), J. Non-Cryst. Solids 348 (2004) 149.
[7] M.H. Lewis, J.M. Johnson, P.S. Bell, J. Am. Ceram. Soc. 62 (1979) 278.
[8] C. Lara, M.J. Pascual, J.M. Prado, A. Duran, Sintering of glasses in the system. RO–Al_2O_3–BaO–SiO_2 (R = Ca, Mg, Zn) studied by hot-stage microscopy, Solid State Ionics 170 (2004) 201.
[9] Ruifang Wang, Zhe Lu, Chaoqian Liu, Ruibin Zhu, Xiqiang Huang, Bo Wei, Na Ai, Wenhui Su, Characteristics of a SiO_2-B_2O_3-Al_2O_3–$BaCO_3$–PbO_2–ZnO glass–ceramic sealant for SOFCs, J. Alloys Compd. 432 (2007) 189.
[10] N. Lahl, K. Singh, L. Singheiser, K. Hilpert, Crystallisation kinetics in AO–Al_2O_3–SiO_2–B_2O_3 glasses (A = Ba, Ca, Mg), J. Mater. Sci. 35 (2000) 3089.
[11] A. Arora, A. Goel, E.R. Shaaban, K. Singh, O.P. Pandey, J.M.F. Ferreira, Crystallization kinetics of BaO–ZnO–Al_2O_3-B_2O_3–SiO_2 glass, Phys. B Cond. Matter 403 (2008) 1738.
[12] S. Mahadevan, A. Giridhar, A.K. Singh, J. Non-Cryst. Solids 88 (1986) 11.
[13] M. Saad, M. Poulin, Mater. Sci. Forum 19–20 (1987) 11.
[14] R. Bohmer, K.L. Nagi, C.A. Angell, D.J. Plazek, Nonexponential relaxations in strong and fragile glass formers, J. Chem. Phys. 99 (1993) 4201.
[15] K. Chebli, J.M. Saiter, J. Grenet, A. Hamou, G. Saffarini, Strong-fragile glass forming liquid concept applied to GeTe chalcogenide glasses, Physica B 304 (2001) 228.
[16] M.M. Wakkad, E.K. Shok, S.H. Mohamed, J. Non-Cryst. Solids 265 (2000) 157.
[17] T.A. Viglis, Strong and fragile glasses: a powerful classification and its consequences, Phys. Rev. B 47 (1993) 2882.
[18] R. Bohmer, C.A. Angell, in: R. Richert, A. Blumen (Eds.), Correlations of the Nonexponentiality and State Dependence of Mechanical Relaxations with Bond Connectivity in Ge-As-supercooled Liquids, Springer, Berlin, 1994, p. 10091.
[19] N.F. Mott, R.W. Gurney, Recent theories of the liquid state, Rep. Prog. Phys. 5 (1938) 46.
[20] R.G. Beaman, J. Polym. Sci 9 (1952) 470.
[21] S. Sakka, J.D. Mackenzie, Relation between apparent glass transition temperature and liquids temperature for inorganic glasses, J. Non-Cryst. Solids 6 (1971) 145.
[22] P. Saswati Ghosh, A. Kundu, R.N. Das Sharma, H.S. Basu, Maiti Microstructure and property evaluation of barium aluminosilicate glass–ceramic sealant for anode-supported solid oxide fuel cell, J. Eur. Ceram. Soc. 28 (2008) 69–76.
[23] G.S. Fulcher, The usefulness of analytic abstracts, J. Am. Ceram. Soc. 8 (1925) 39.
[24] L. Blum, R. Fleck, Jansing, High-temperature fuel cell and high-temperature fuel cell stack US Patent 6165632 (2000).
[25] Vishal Kumar, A. Arora, O.P. Pandey, K. Singh, Studies on thermal and structural properties of glasses as sealants for solid oxide fuel cells, Int. J. Hydrogen Energy 33 (1) (2008) 434.
[26] Vishal Kumar, Sarita Sharma, O.P. Pandey, K Singh, Thermal and physical properties of $30SrO–40SiO_2–20B_2O_3–10A_2O_3$ (A = La, Y, Al) glasses and their chemical reaction with bismuth vanadate for SOFC, Solid State Ionics 181 (2010) 79.
[27] J. Vázquez, C. Wagner, P. Villares, R Jim!enez Garay, A theoretical method for determining the crystallized fraction and kinetic parameters by DSC, using non-isothermal techniques, J. Non-Cryst. Solids 235 (1998) 548.
[28] A. Arora, E.R. Shaaban, K. Singh, O.P. Pandey, Crystallization kinetics of BaO–ZnO–Al_2O_3-B_2O_3–SiO_2 glass, J. Non-Cryst. Solids 354 (2008) 3944.
[29] K. Singh, Neha Gupta, O.P. Pandey, Effect of Y_2O_3 on the crystallization behavior of SiO_2–MgO–B_2O_3–Al_2O_3 glasses, J. Mater. Sci. 42 (2007) 6426.